Received: 3 February 2024 | Revised: 5 March 2024 | Accepted: 28 March 2024

DOI: 10.1111/jon.13201

JOURNAL OF NEUROIMAGING
THE OFFICIAL JOURNAL OF THE AMERICAN SOCIETY OF NEUROIMAGING
WILEY

CLINICAL INVESTIGATIVE STUDY

Detection of pathological contrast enhancement with synthetic brain imaging from quantitative multiparametric MRI

Graziella Donatelli[1,2] | Gianmichele Migaleddu[1] | Matteo Cencini[3] | Paolo Cecchi[1,2] | Claudio D'Amelio[4] | Luca Peretti[2,5] | Guido Buonincontri[5] | Michela Tosetti[5] | Mauro Costagli[5,6] | Mirco Cosottini[4]

[1]Neuroradiology Unit, Azienda Ospedaliero-Universitaria Pisana, Pisa, Italy

[2]Imago7 Research Foundation, Pisa, Italy

[3]Pisa Division, National Institute for Nuclear Physics (INFN), Pisa, Italy

[4]Neuroradiology Unit, Department of Translational Research on New Technologies in Medicine and Surgery, University of Pisa, Pisa, Italy

[5]Laboratory of Medical Physics and Magnetic Resonance, IRCCS Fondazione Stella Maris, Pisa, Italy

[6]Department of Neuroscience, Rehabilitation, Ophthalmology, Genetics, Maternal and Child Sciences (DINOGMI), University of Genoa, Genoa, Italy

Correspondence
Mirco Cosottini, Neuroradiology Unit, Azienda Ospedaliero-Universitaria Pisana, Via Paradisa 2, 56124 Pisa, Italy.
Email: mirco.cosottini@unipi.it

Mauro Costagli, Laboratory of Medical Physics and Magnetic Resonance, IRCCS Stella Maris, Via del Tirreno 341, 56128 Pisa, Italy.
Email: mauro.costagli@fsm.unipi.it

Funding information
Italian Ministry of Health, Grant/Award Number: GR-2016-02361693

Abstract

Background and Purpose: We aimed to test whether synthetic T1-weighted imaging derived from a post-contrast Quantitative Transient-state Imaging (QTI) acquisition enabled revealing pathological contrast enhancement in intracranial lesions.

Methods: The analysis included 141 patients who underwent a 3 Tesla-MRI brain exam with intravenous contrast media administration, with the post-contrast acquisition protocol comprising a three-dimensional fast spoiled gradient echo (FSPGR) sequence and a QTI acquisition. Synthetic T1-weighted images were generated from QTI-derived quantitative maps of relaxation times and proton density. Two neuroradiologists assessed synthetic and conventional post-contrast T1-weighted images for the presence and pattern of pathological contrast enhancement in intracranial lesions. Enhancement volumes were quantitatively compared.

Results: Using conventional imaging as a reference, synthetic T1-weighted imaging was 93% sensitive in revealing the presence of contrast enhancing lesions. The agreement for the presence/absence of contrast enhancement was almost perfect both between readers ($k = 1$ for both conventional and synthetic imaging) and between sequences ($k = 0.98$ for both readers). In 91% of lesions, synthetic T1-weighted imaging showed the same pattern of contrast enhancement visible in conventional imaging. Differences in enhancement pattern in the remaining lesions can be due to the lower spatial resolution and the longer acquisition delay from contrast media administration of QTI compared to FSPGR. Overall, enhancement volumes appeared larger in synthetic imaging.

Conclusions: QTI-derived post-contrast synthetic T1-weighted imaging captures pathological contrast enhancement in most intracranial enhancing lesions. Further comparative studies employing quantitative imaging with higher spatial resolution is needed to support our data and explore possible future applications in clinical trials.

Mauro Costagli and Mirco Cosottini contributed equally to this work and should be considered as co-last authors.

KEYWORDS
contrast enhancement, magnetic resonance imaging, quantitative transient-state imaging, synthetic imaging

INTRODUCTION

T1-weighted (T1-w) imaging acquired after the intravenous administration of paramagnetic contrast media is widely used in clinical practice to assess patients with different disorders of the central nervous system, including tumors and inflammatory, demyelinating, and infectious diseases.[1] Gadolinium-based contrast agents have an intravascular extracellular distribution and do not cross either cell membranes or the intact blood-brain barrier.[2] When injected during an MRI exam, post-contrast T1-w imaging is able to reveal indirectly the contrast media extravasation across the wall of vessels with no or impaired blood-brain barrier properties and the possible hypervascularity of intra- and extra-axial lesions. Both conditions are depicted as areas of signal hyperintensity due to the contrast-related shortening of the T1 relaxation time of water protons near contrast media molecules.[3]

MRI is a fundamental, noninvasive diagnostic tool used to study the central nervous system due to its ability to provide a multiparametric description of tissue properties and unprecedented tissue contrast without the use of ionizing radiation. It is considered essential in the diagnosis of many brain disorders. From the introduction of paramagnetic contrast media in the mid-1980s, intravenous paramagnetic contrast media have been increasingly used to improve diagnostic accuracy in selected cases,[4] in the decision-making process for treatment, in guiding stereotactic biopsy and radiosurgery,[5] in estimating tumor grading,[6] and in monitoring effectiveness and possible complications of therapies.[7] Post-contrast T1-w imaging has also been proven to be able to reveal small enhancing lesions undetectable in unenhanced MRI because of their location, very small dimensions, and/or their lack of mass effect or visible edema, such as small brain metastasis.[8]

Besides conventional sequences, post-contrast synthetic T1-w images could also serve to assess enhancing lesions. In the last decade, a number of primarily quantitative MRI techniques able to quantify multiple tissue parameters in a single acquisition have been developed. Among these techniques, MR Fingerprinting[9] and Quantitative Transient-state Imaging (QTI)[10] have progressively received attention as they provide repeatable and reproducible quantitative maps of different tissue properties in clinically feasible acquisition times and at competitive spatial resolutions.[11] Additionally, by using quantitative maps as entries of appropriate mathematical formulae, it is possible to synthesize images with multiple tissue contrasts similar to those used in a clinical routine.[12]

To the best of our knowledge, the systematic comparison between conventional and three-dimensional (3D) QTI-derived synthetic imaging in depicting and characterizing brain lesions is still missing. Therefore, in this study, we explored one of the potential applications of synthetic imaging in the clinical setting: we tested whether synthetic T1-w images obtained from 3D QTI on a 3T scanner were able to reveal pathological contrast enhancement in intra- and extra-axial lesions in a wide cohort of patients with different brain diseases and neurological symptoms.

METHODS

Patients

We included in this study all of the adult patients enrolled in the prospective study "GR-2016-02361693" between March 2019 and December 2021, who underwent an MRI exam of the brain with contrast media administration and whose MRI protocol comprised a post-contrast 3D fast spoiled gradient echo (FSPGR) acquisition (Figure 1). Patients were referred to the Neuroradiology Unit to characterize brain lesions, monitor diseases, or search for possible physical causes of reported neurological signs and symptoms. The study was approved by the local ethics committee and all patients gave their written informed consent to participate.

Data acquisition and post-processing

All the acquisitions were performed on a 3T MR system (MR750 scanner, GE Healthcare) equipped with an 8-channel head coil and consisted of a clinical and an experimental protocol.

The clinical protocol included two 3D T1-w FSPGR sequences acquired before (Time of Repetition [TR] = 8.2 milliseconds, Time of Echo [TE] = 3.2 milliseconds, inversion time = 450 milliseconds, Flip Angle [FA] = 8°, spatial resolution = $1 \times 1 \times 1$ mm^3) and after (TR = 8 milliseconds, TE = 3.2, FA = 12°, field of view = 240 mm, matrix size = 256×256, images reconstructed with voxel size of $0.5 \times 0.5 \times 0.5$ mm^3) contrast media administration.

The experimental protocol included two QTI acquisitions,[10,13] one performed before contrast media administration, and one after, at the end of the clinical protocol. The QTI implementation details and scanning parameters used in this study were previously described in detail.[14] In short, each QTI consisted of an inversion-prepared 3D steady-state free precession acquisition with 3D spiral trajectory for k-space sampling with TE/TR = 0.5/8.5 milliseconds, variable FA train for T1 and T2 encoding, covering the whole head with a field of view of 225 and 1.125 mm isotropic voxels in 7 minutes. Quantitative maps of relaxation times T1 and T2 and proton density (PD) were obtained using a neural network trained with a pre-computed dictionary of MR

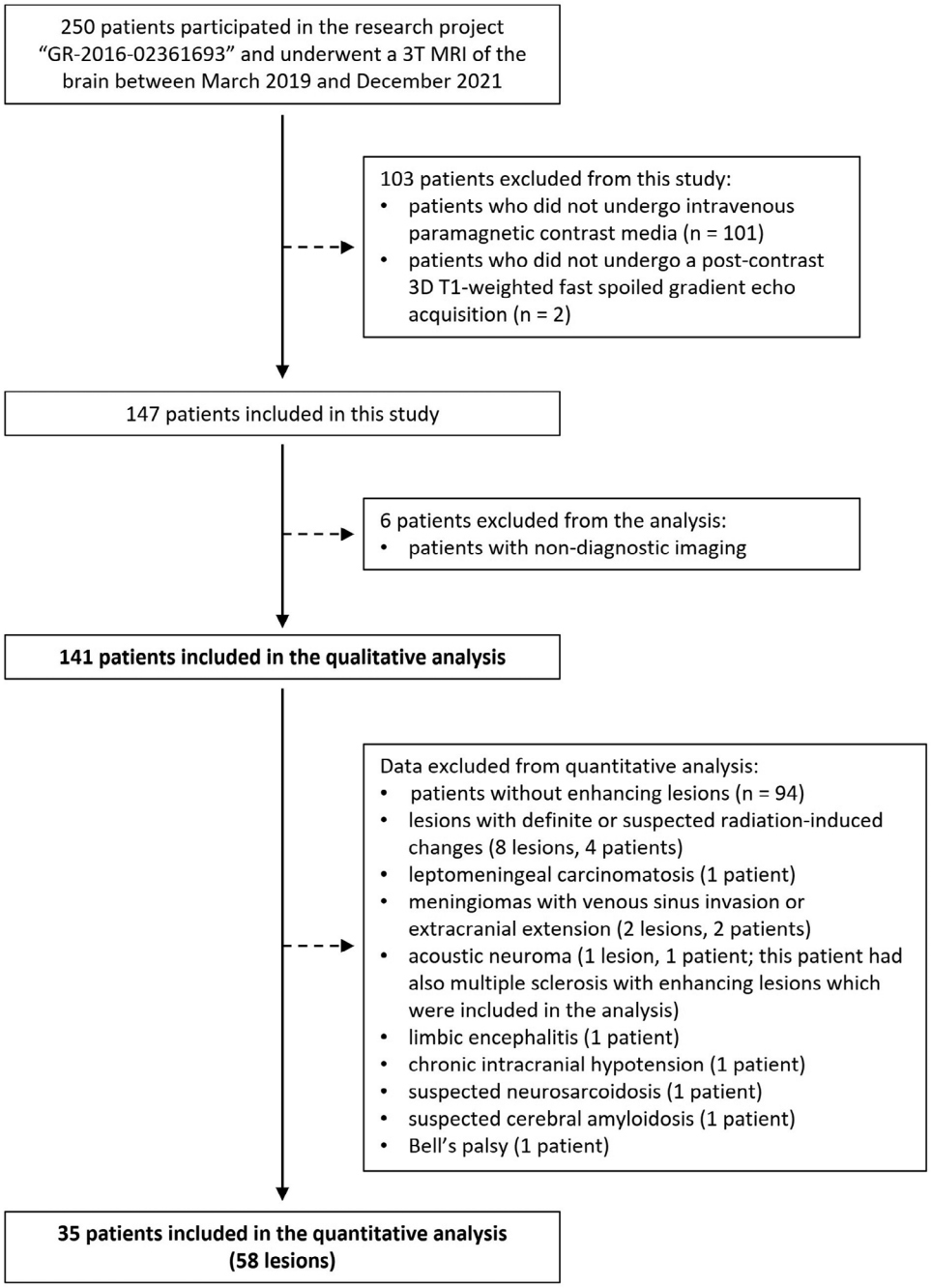

FIGURE 1 Flow chart of study participants. *n*, number of patients; 3D, three-dimensional; 3T, 3 Tesla.

signal evolutions.[10] Then, synthetic T1-w images simulating Gradient Recalled Echo were synthesized from the T1 and PD maps using the open-source software PySynthMRI (v1.0.0, IRCCS Stella Maris, Pisa, Italy, https://github.com/FiRMLAB-Pisa/pySynthMRI)[12] according to the equation S = PD*[1−exp(−TR/T1)], where S is the signal of each voxel and the TR was set to 113 milliseconds.

As the delay between contrast administration and MR acquisitions differed for conventional and QTI sequences, the time gap between the two post-contrast acquisitions was recorded.

DATA ANALYSIS

Qualitative analysis

Pre- and post-contrast conventional and synthetic T1-w images were visually inspected by two neuroradiologists to determine the possible presence of contrast enhancing tissue, the number of enhancing lesions, and the enhancement pattern. Then, the recorded information was compared between synthetic and conventional imaging.

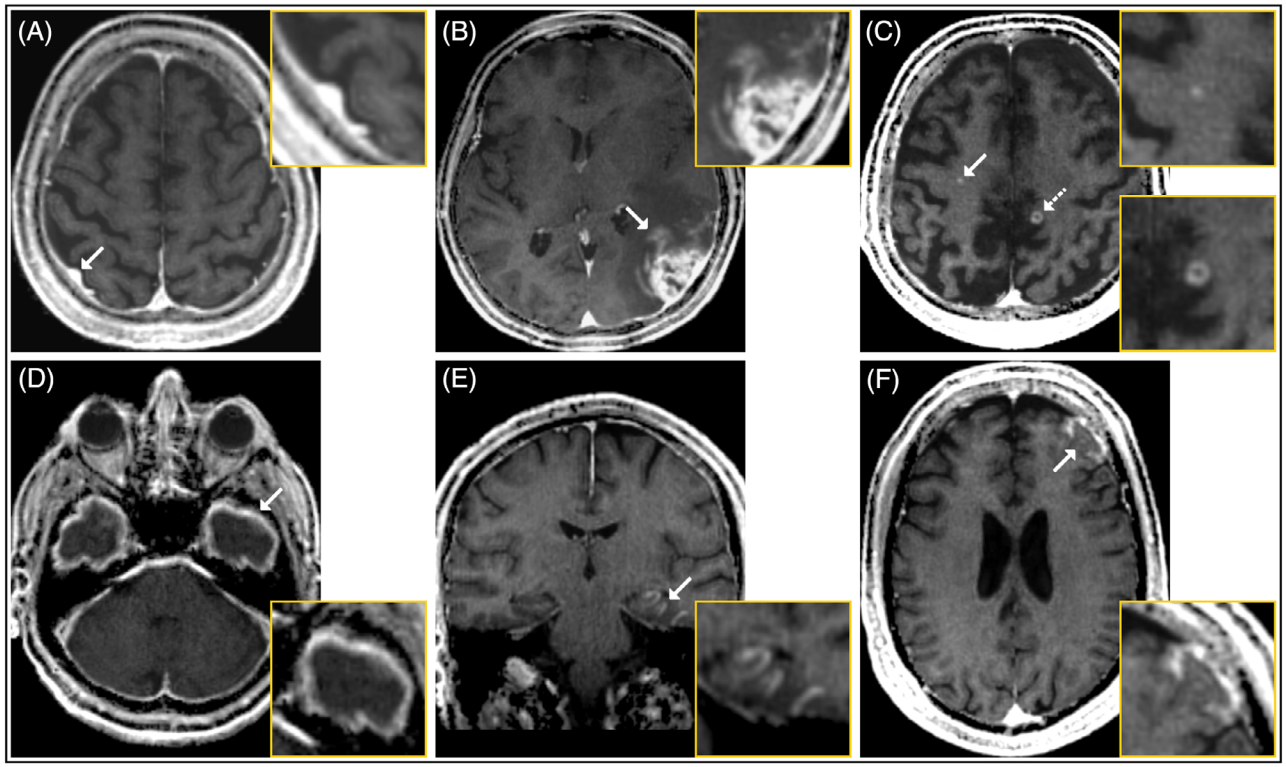

FIGURE 2 Examples of different patterns of contrast enhancement with the corresponding magnified views in yellow boxes. (A) Homogeneous enhancement in a meningioma (arrow). (B) Inhomogeneous enhancement in a primary intra-axial brain tumor (arrow). (C) Punctiform (arrow) and ring-like (dashed arrow) enhancement in two brain metastases. (D) Ribbon-like enhancement of the thickened pachymeninges (arrow) in a patient with chronic intracranial hypotension. (E) Gyriform cortical enhancement (arrow) in a patient with limbic encephalitis. (F) Gyriform leptomeningeal enhancement (arrow) in a patient suspected to have leptomeningeal carcinomatosis.

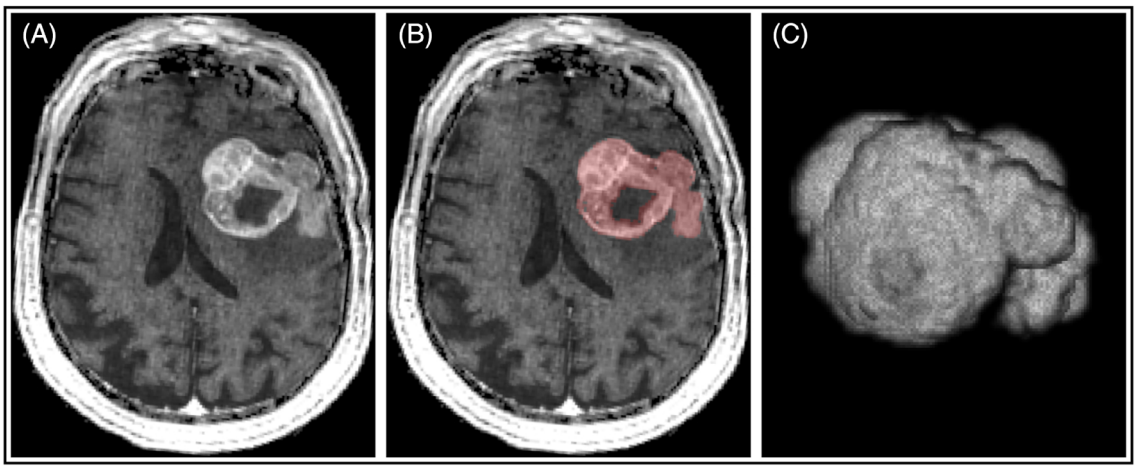

FIGURE 3 Example of lesion segmentation on synthetic images. The pathological enhancing tissue was detected (A) and segmented on post-contrast T1-weighted images (light red in B). Panel C shows the volume rendering of the segmented lesion.

First, one of the readers assessed the overall quality of synthetic and conventional T1-w images. Scans including at least one T1-w image, either conventional or synthetic, of nondiagnostic quality were excluded from the following steps. Then, neuroradiologists assessed the images and recorded the series in which they noted the presence of pathologically enhancing intracranial tissue. They worked individually and assessed images in two separate sessions, with scans presented in random order and synthetic images evaluated in the first reading session. The agreement for the presence/absence of pathological enhancing lesions was computed between conven-

TABLE 1 Distribution of enhancing lesions across diagnostic categories in both conventional and synthetic T1-weighted imaging.

	Conventional T1-weighed imaging		Synthetic T1-weighted imaging	
	Number of patients with enhancing lesions	Number of enhancing lesions	Number of patients with enhancing lesions	Number of enhancing lesions
Primary intra-axial brain tumors[a]	18	18	18	18
Extra-axial tumors	16	18	15	16
Secondary tumors	6	18	6	19
Multiple sclerosis	5	22	5	18
Limbic encephalitis[a]	1	1	1	1
Chronic intracranial hypotension[a]	1	1	1	1
Suspected neurosarcoidosis[a]	1	1	1	1
Suspected cerebral amyloidosis[a]	1	1	1	1
Bell's palsy[a]	1	1	1	1

[a]As these lesions can show multiple areas of contrast enhancement, they were considered as part of the same alteration.

TABLE 2 Results of quantitative analysis.

		Volume of lesions[a]		
	Number of lesions	Conventional T1-weighted imaging	Synthetic T1-weighted imaging	*p*-value
All lesions	58	142 (1336) [6-63,508]	147 (1758) [10-73,626]	< .0001
Primary intra-axial brain tumors	16	1914 (11,200) [9-63,508]	1677 (14,815) [24-73,626]	< .01
Meningiomas	13	802 (2164) [81-4085]	668 (2438) [90-3880]	> .05
Secondary intra-axial tumors	11	16 (131) [6-10,795]	66 (137) [11-10,532]	> .05
Demyelinating multiple sclerosis lesions	18	19 (29) [7-786]	42 (50) [10-3007]	< .0001

[a]Expressed in cubic millimeters as: median (interquartile range) [range].

tional and synthetic imaging and between readers using the Cohen's kappa coefficient. Subsequently, the readers jointly counted enhancing lesions in both synthetic and conventional imaging and classified pathological enhancement according to morphology in the following seven types: homogeneous, inhomogeneous, punctiform, ring-like, ribbon-like, gyriform cortical, and gyriform leptomeningeal (Figure 2).

Enhancing lesions were then diagnosed based on clinical data, conventional imaging and, when available, pathological information emerging from patient interview and data stored in the hospital database.

Quantitative analysis

Intra- and extra-axial tissue areas of pathological contrast enhancement were identified as T1 hyperintense regions and segmented by a neuroradiologist separately on conventional and synthetic post-contrast T1-w images using a semi-automated segmentation technique based on user-supervised local thresholding (FSLeyes v0.22.6, FMRIB Centre, Oxford, UK, https://fsl.fmrib.ox.ac.uk/fsl/fslwiki/FSLeyes) (Figure 3). To avoid bias related to differences in voxel sizes, FSPGR datasets used for the quantitative analysis were resampled to the same resolution of the synthetic images. Then, the

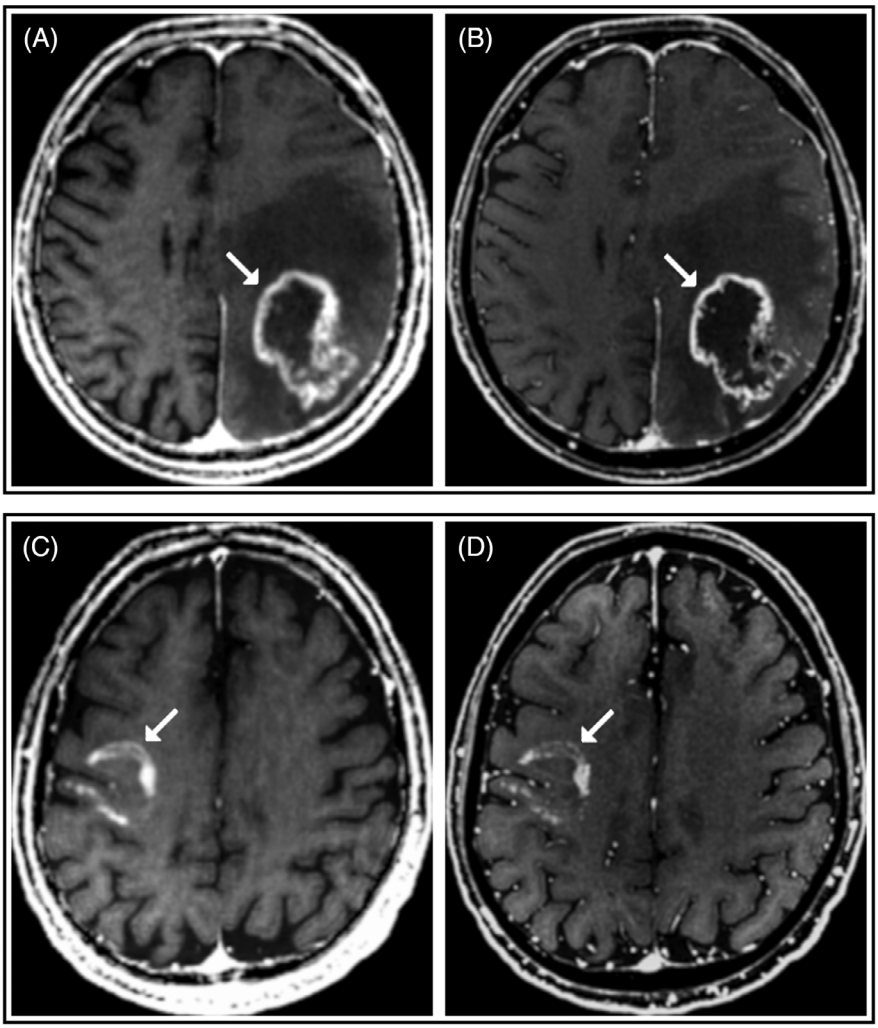

FIGURE 4 Synthetic (A and C) and conventional (B and D) post-contrast T1-weighted images in two patients with intra-axial brain tumors. Panels A and B show images of a patient with a large glioblastoma involving parietal, temporal, and occipital lobes of the left hemisphere. Panels C and D show images of a patient with a diffuse astrocytoma in the frontal and parietal lobes of the right hemisphere. In both patients, synthetic imaging (A and C) reveals the pathological enhancement of the tumoral mass (arrows) and reflects the inhomogeneous pattern of enhancement visible at conventional imaging (arrows in B and D).

volume of enhancing tissue was extracted from conventional and synthetic images and compared with each other using the Wilcoxon matched-pairs signed rank test, with the significance level set to 5%.

This analysis only included: primary and secondary intra-axial brain tumors with no definite or suspected radiation-induced changes, meningiomas without venous sinus invasion or extracranial extension, and multiple sclerosis lesions (Figure 1). This strategy was adopted in order to ensure homogeneous groups of lesions and avoid challenging segmentation (ie, gyriform and ribbon-like contrast-enhanced areas).

RESULTS

One hundred and forty-seven patients were included in the study; 73 were males and 74 were females, aged 53 ± 16 years old (range 21-84). Among them, six scans were excluded because of nondiagnostic imaging and the remaining 141 scans were included in the analysis (Figure 1).

Upon radiological inspection of the images, 47 patients had contrast enhancing lesions in conventional imaging (81 lesions overall) and 46 patients had enhancing lesions in synthetic imaging (76 lesions overall; one enhancing lesion was visible only in synthetic imaging). Synthetic T1-w images showed contrast enhancement in 93% of enhancing lesions visible in conventional imaging.

The agreement for the presence/absence of pathological intracranial contrast enhancement was almost perfect both between readers ($k = 1$ for both sequences) and between sequences ($k = 0.98$ for both readers).

Patients with enhancing lesions had one or more of the following: previous or current primary intra-axial brain tumors, extra-axial tumors (including meningiomas and one acoustic neuroma), secondary tumors (including brain metastasis and one patient with suspected

leptomeningeal carcinomatosis), multiple sclerosis, limbic encephalitis, chronic intracranial hypotension, suspected neurosarcoidosis, suspected cerebral amyloidosis, and Bell's palsy. In the group of intra-axial brain tumors, there were two patients treated for a glioblastoma multiforme who had imaging changes suspected of radiation-induced alterations, as diagnosed with advanced conventional sequences, and two patients with melanoma or lung cancer who had radionecrotic brain lesions confirmed at follow up. Three patients had two different diseases with enhancing components: one patient had multiple sclerosis and an acoustic neuroma confined within the internal auditory canal, and two patients had a primary intra-axial brain tumor and a meningioma each. The distribution of enhancing lesions across diagnostic categories in both conventional and synthetic T1-w imaging is reported in Table 1, and examples of conventional versus synthetic comparative post-contrast T1-w imaging are shown in Figures 4–8.

Enhancing lesions missed in T1-w synthetic imaging were small (four demyelinating lesions, 2 mL each, Figure 9A,B), small and close to basicranium (a meningioma at the level of the jugum sphenoidale, Figure 9C,D) or close to basicranium and large arteries (a meningioma at the level of the cavernous sinus, Figure 9E,F).

Synthetic T1-w images showed the same pattern of contrast enhancement visible in conventional imaging in 68 out of 75 lesions (91%) detected with both techniques. In one primary intra-axial brain tumor, the multiple ring-like components visible at conventional imaging changed into an inhomogeneously enhancing area at synthetic imaging. Three lesions with inhomogeneous enhancement at conventional imaging showed homogeneous enhancement in synthetic post-contrast T1-w images (two extra-axial tumors and one demyelinating multiple sclerosis lesion). Three ring-enhancing lesions at conventional imaging showed homogeneous enhancement in synthetic post-contrast T1-w images (two brain metastasis and one demyelinating plaque).

Fifty-eight lesions were included in the quantitative analysis. The enhancing tissue volume computed on synthetic imaging was significantly higher than that measured on conventional imaging in primary intra-axial brain tumors and in demyelinating lesions (Table 2). There were no significant differences at the group level for meningiomas or secondary brain tumors.

The average time elapsed between post-contrast 3D FSPGR and QTI acquisitions was 8 minutes.

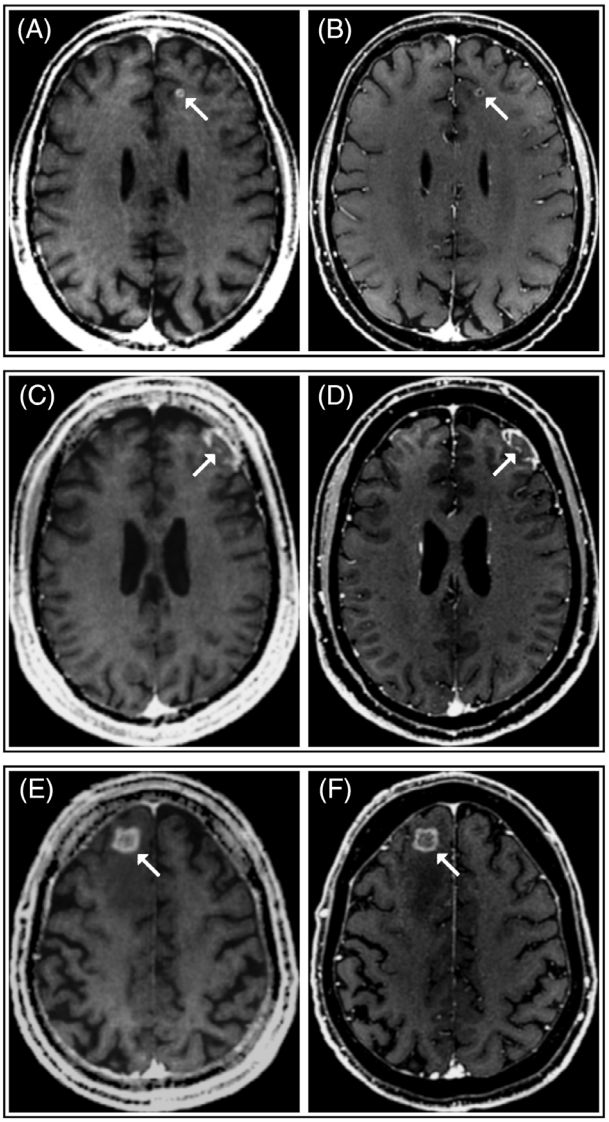

FIGURE 5 Synthetic (A, C, and E) and conventional (B, D, and F) post-contrast T1-weighted images in two patients with brain metastases and one patient with radionecrosis. Panels A and B show images of a patient with non-small cell lung cancer and an intra-axial metastasis in the left frontal lobe (arrows). Panels C and D show images of a patient with history of metastatic melanoma and a suspected leptomeningeal carcinomatosis (arrows). Panels E and F show images of a patient with melanoma and the radiological suspicion of radiation necrosis (arrows) following radiotherapy of brain metastasis. In all these patients, synthetic imaging revealed the same pattern of contrast enhancement visible in conventional imaging (ring-like in A and E, and gyriform leptomeningeal in C).

DISCUSSION

In this study, we tested whether post-contrast synthetic T1-w images of the brain derived from a 3D QTI acquisition were able to reveal intra- and extra-axial pathological enhancing lesions using conventional imaging as a reference. We found that synthetic imaging was 93% sensitive in revealing enhancing lesions, which enabled the identification of pathological contrast enhancement in 98% of patients, and confirmed the pattern of enhancement in 91% of lesions. Furthermore, the volume of pathologically enhancing tissue was greater in synthetic than in conventional imaging in primary intra-axial brain tumors and in demyelinating lesions, whereas the difference was not statistically significant at the group level for secondary intra-axial tumors or for meningiomas.

When interpreting the results of this study, it should be considered that two factors, combined with each other, are responsible for the contrast agent kinetic in each group of lesions. First, pathological contrast enhancement relies on two mechanisms: the increased volume of contrast-enhanced blood in vessels because of neovascular-

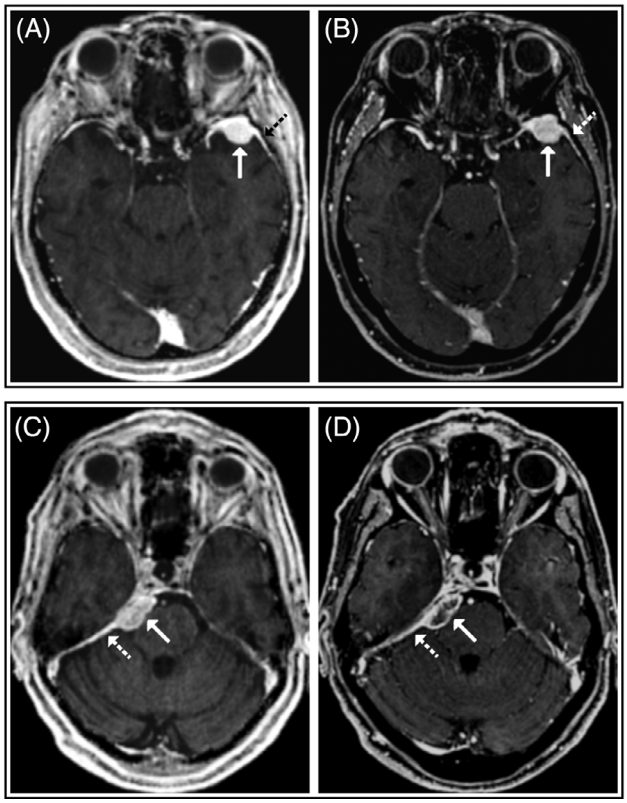

FIGURE 6 Synthetic (A and C) and conventional (B and D) post-contrast T1-weighted images in two patients with meningioma, one at the level of the greater wing of the left sphenoid bone (arrows in A and B), the other at the level of the pyramid of the right temporal bone (arrows in C and D). In both cases, synthetic imaging clearly revealed the presence of intensely enhancing extra-axial masses (arrows) and the respective dural tails (black and white dashed arrows). In one patient (A-B), the pattern of contrast enhancement was homogeneous in both synthetic (A) and conventional (B) imaging. In the other patient (C-D), the pattern of contrast enhancement was inhomogeneous in synthetic (C) and even more in conventional (D) imaging.

ity (as in tumors) or vasodilatation (as in the intracranial hypotension syndrome), and the contrast media accumulation in the extravascular extracellular space because of a disrupted (as in intra-axial lesions) or missing (as in extra-axial and pachymeningeal alterations) blood-brain barrier, the latter depending in turn on the balance between vascular leakage and extracellular clearance of contrast media.[15] Second, in some disorders, the acquisition delay from contrast media administration influences number, size, signal intensity, and pattern of enhancing lesions because in delayed imaging more time is allowed for the contrast media to cross an impaired blood-brain barrier and spread within the extracellular compartment.

In intra-axial tumors, the increased microvascular permeability (and the consequent contrast enhancement) results from molecular and morphological alterations of the blood-brain barrier components which compromise its structural integrity.[16–18] In primary neoplasms, the presence and degree of blood-brain barrier disruption and angiogenesis can be heterogeneous within tumor volume and differ with

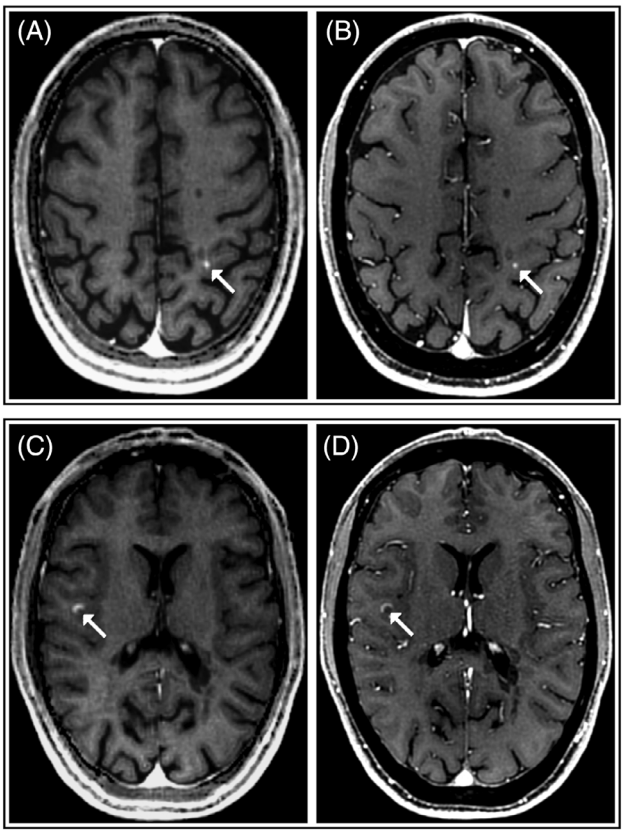

FIGURE 7 Synthetic (A and C) and conventional (B and D) post-contrast T1-weighted images in a patient with relapsing-remitting multiple sclerosis. Two enhancing demyelinating lesions are visible in the white matter in both datasets: one punctiform plaque with homogeneous enhancement in the left superior parietal lobule (arrows in A and B), and one lesion with incomplete ring-like enhancement in the right frontal operculum (arrows in C and D).

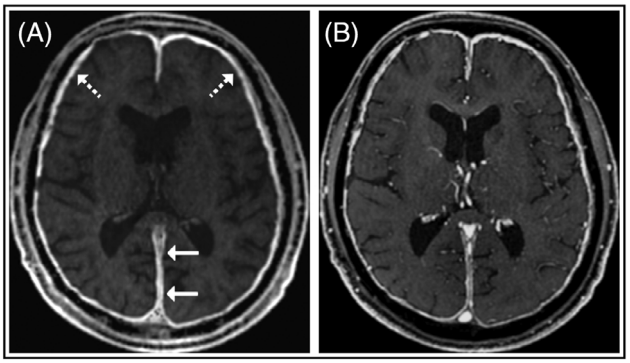

FIGURE 8 Synthetic (A) and conventional (B) post-contrast T1-weighted images in a patient with chronic intracranial hypotension. The intense, ribbon-like contrast enhancement of thickened pachymeninges, a typical finding of this condition, is appreciable in synthetic imaging in both the pachymeninges up against the inner table of the skull (dashed arrows in A) and at the level of dural reflections of the falx cerebri (arrows in A).

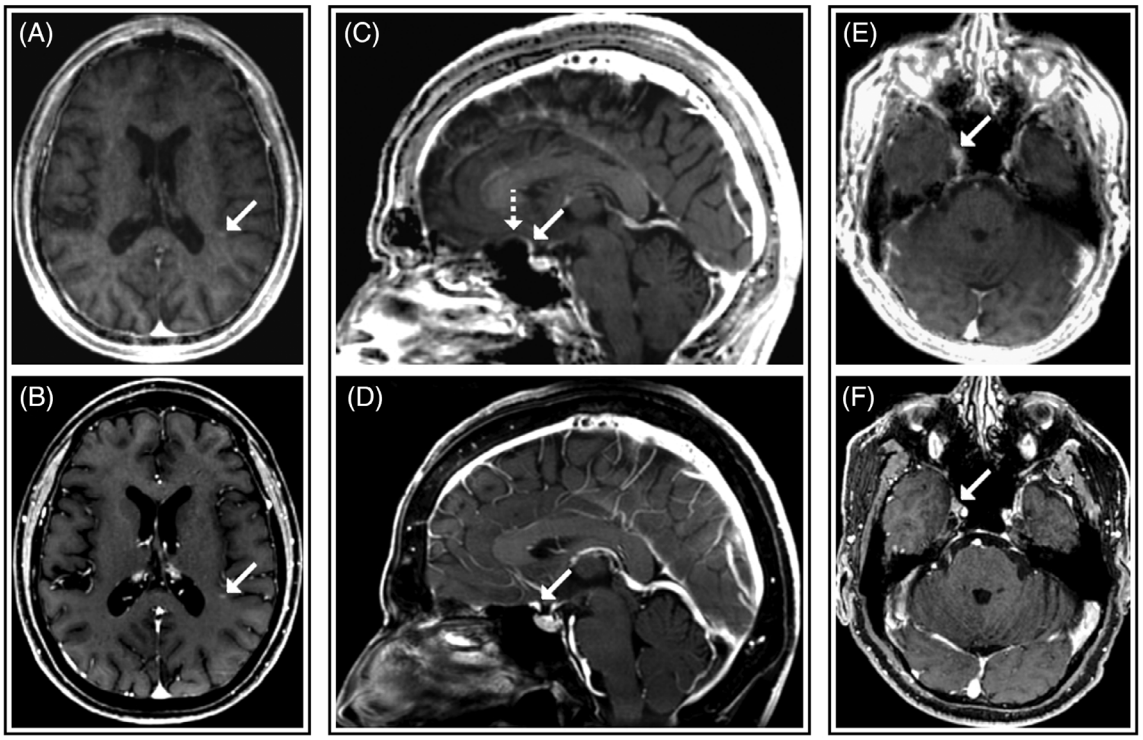

FIGURE 9 Examples of discrepancies in enhancing lesions visibility between synthetic (A, C, and E) and conventional (B, D, and F) post-contrast T1-weighted imaging. A-B: Contrast enhancing demyelinating lesion in a patient with multiple sclerosis (arrows). The small lesion was visible in conventional images but failed to be detected in synthetic images. C-D: Meningioma at the level of the jugum sphenoidale (arrows) visible in conventional images (D) but missed in the blinded assessment of synthetic images (C); in the latter, the artifact at the air-tissue interface (dashed arrow in C) reduced the lesion conspicuity. E-F: Meningioma at the level of the cavernous sinus (arrows). The lower spatial resolution of synthetic images (E) reduced the visibility of the lesion, which was not clearly distinguished from the internal carotid artery.

type and grade.[17,19] In our study, we found that the volume of enhancing tissue was greater in synthetic than in conventional imaging and the enhancement pattern was confirmed in all but one case. The enhancing volume increase with increasing acquisition delay after contrast media injection, reported also in previous studies,[20] probably depends on the extravascular accumulation of a greater amount of contrast media, as more time is allowed for it to cross the impaired blood-brain barrier, also in areas with a low degree of disruption, and spread through the edematous extracellular compartment.[21] In brain metastasis, instead, the volume of enhancing tissue did not significantly differ between techniques at the group level. This finding is in line with previous studies that did not report a definite difference in lesion detection and conspicuity between early and delayed postcontrast T1-w imaging,[8] although some metastases can show a greater enhancing area in delayed imaging.[22] In our series, one lesion was detected only in synthetic imaging and two lesions changed the enhancement pattern from ring-like in conventional to homogeneous in synthetic imaging, the latter possibly ascribable to the coarser resolution of synthetic images, as discussed below.

Meningiomas usually have a strong and rapid enhancement[23] probably reflecting the high vascularity, which is a characteristic of some subtypes,[24] and the lack of a barrier phenomenon.[25] However, different subtypes of meningiomas have different kinetics of contrast enhancement: angioblastic meningiomas are markedly hypervascular and meningoendothelial meningiomas have a poor extracellular matrix which may allow a rapid contrast enhancement; on the other hand, fibrous meningiomas have an abundant extracellular matrix which can prevent the prompt contrast enhancement, and transitional meningiomas show variable dynamic patterns depending on the specific tissue composition.[23] The similarity in the volume of enhancing meningioma tissue measured with the two techniques suggests that most meningiomas in our series have an increased vascularity and/or a poor extracellular matrix. Synthetic imaging also proved able to reveal the "dural tail" (Figure 5), that is the thickened and early enhancing dura mater in continuity with the meningioma and mostly representing an inflammatory dural reaction,[26] but failed to depict two small meningiomas: one was contiguous to the jugum sphenoidale, where the artifact at the air-tissue interface reduced the lesion conspicuity; the other was at the level of the cavernous sinus and blended with the adjacent internal carotid artery probably because of the insufficient spatial resolution of images.

In patients with multiple sclerosis, contrast enhancement is associated with inflammation,[27,28] and depends on the contrast media leakage across a disrupted blood-brain barrier[27] and its accumulation in the extravascular extracellular space. In our study, four out of 22 enhancing lesions recorded in conventional imaging were not visible in synthetic imaging, probably because their sizes were too small to be detected with the QTI implementation we used. Considering

the 18 lesions detected in both imaging types, the overall increase in lesion volume that we found in synthetic imaging can be ascribed to the delay between contrast administration and image acquisition. This observation is in agreement with a previous study where, moving from early to delayed scans, the size of enhancing demyelinating lesions was shown to increase.[29] Results of pattern analysis can be interpreted in view of the concept that small nodular plaques with centrifugal enhancement are expected to show a wider enhancing volume over time without changing the shape of tissue enhancement, whereas ring-like lesions with centripetal enhancement tend to fill in in delayed scans and become homogeneous nodular enhancing plaques.[30] Indeed, in our study, all lesions with punctiform or homogeneous enhancement at conventional imaging had their pattern confirmed in the delayed synthetic imaging, and two lesions inhomogeneously or ring-like enhancing at conventional imaging showed homogeneous enhancement at synthetic imaging.

In the patient with chronic intracranial hypotension, the enhancement of thickened pachymeninges, usually early and intense, is clearly appreciable in synthetic imaging. It is probably due to the increased concentration of contrast media in dural veins, which are dilated as a consequence of the reduced volume of cerebrospinal fluid, and to its accumulation in the interstitial compartment because vessels of the dura matter do not have blood-brain barrier properties.[31]

The main limitation of this study is that, for a rigorous comparison between conventional and synthetic post-contrast T1w imaging, conventional and experimental sequences should have been acquired in two separate MR sessions after an equal delay from the intravenous administration of an identical dose of the same contrast media. Moreover, the time elapsed between the two exams should have been long enough to allow for the complete contrast media wash out but also as short as possible to minimize the risk of biological changes within lesions. However, as this is the first study investigating the ability of 3D QTI-derived synthetic imaging in capturing contrast enhancement in intracranial lesions, such an experimental design would have raised obvious ethical concerns. With the adopted approach, we were able to prove that post-contrast QTI sequences are very sensitive in revealing intracranial lesions with pathological contrast enhancement. Another limitation is that the spatial resolution differed between conventional and synthetic images. For the purpose of this study, we did not resample data used in the qualitative analysis to enable a direct comparison between the experimental sequence and the one optimized and routinely used in the clinical setting.

Our results support the conclusion that QTI-derived post-contrast synthetic T1-w imaging is able to capture pathological contrast enhancement in most intra- and extra-axial enhancing lesions, and encourage further evaluation of this sequence in the clinical research setting. Further comparative studies employing quantitative imaging with higher spatial resolution are needed to support our results and the possible future application of this technique in clinical trials.

ACKNOWLEDGMENTS

The authors thank Dr. Oliver Kiersnowski for his help with refining the English language and grammar in this paper.

Open access funding provided by BIBLIOSAN.

FUNDING INFORMATION

This study is part of a research project (grant n. GR-2016-02361693) funded by the Italian Ministry of Health and co-funded by Tuscany Region. The work has been partially supported also by grant RC and the 5 × 1000 voluntary contributions to IRCCS Fondazione Stella Maris, funded by the Italian Ministry of Health. This study was partially supported also by a research grant from GE HealthCare.

ORCID

Graziella Donatelli https://orcid.org/0000-0002-5325-0746
Gianmichele Migaleddu https://orcid.org/0000-0002-0380-9927
Matteo Cencini https://orcid.org/0000-0001-7060-6305
Paolo Cecchi https://orcid.org/0000-0003-2725-2657
Luca Peretti https://orcid.org/0000-0002-8779-8662
Guido Buonincontri https://orcid.org/0000-0002-8386-639X
Michela Tosetti https://orcid.org/0000-0002-2515-7560
Mauro Costagli https://orcid.org/0000-0001-9073-1082
Mirco Cosottini https://orcid.org/0000-0001-9400-6574

REFERENCES

1. Smirniotopoulos JG, Murphy FM, Rushing EJ, et al. Patterns of contrast enhancement in the brain and meninges. Radiographics. 2007;27:525–51.
2. Weinmann HJ, Brasch RC, Press WR, et al. Characteristics of gadolinium-DTPA complex: a potential NMR contrast agent. Am J Roentgenol. 1984;142:619–24.
3. Bronen RA, Sze G. Magnetic resonance imaging contrast agents: theory and application to the central nervous system. J Neurosurg. 1990;73:820–39.
4. Runge VM, Schaible TF, Goldstein HA, et al. Gd DTPA. Clinical efficacy. Radiographics. 1988;8:147–59.
5. Donahue BR, Goldberg JD, Golfinos JG, et al. Importance of MR technique for stereotactic radiosurgery. Neuro Oncol. 2003;5:268–74.
6. Tovi M, Lilja A, Bergström M, et al. Delineation of gliomas with magnetic resonance imaging using Gd-DTPA in comparison with computed tomography and positron emission tomography. Acta Radiol. 1990;31:417–29.
7. Yoshii Y, Komatsu Y, Yamada T, et al. Malignancy and viability of intraparenchymal brain tumours: correlation between Gd-DTPA contrast MR images and proliferative potentials. Acta Neurochir (Wien). 1992;117:187–94.
8. Sze G, Milano E, Johnson C, et al. Detection of brain metastases: comparison of contrast-enhanced MR with unenhanced MR and enhanced CT. Am J Neuroradiol. 1990;11:785–91.
9. Ma D, Gulani V, Seiberlich N, et al. Magnetic resonance fingerprinting. Nature. 2013;495:187–92.
10. Gómez PA, Cencini M, Golbabaee M, et al. Rapid three-dimensional multiparametric MRI with quantitative transient-state imaging. Sci Rep. 2020;10:1–17.
11. Buonincontri G, Kurzawski JW, Kaggie JD, et al. Three dimensional MRF obtains highly repeatable and reproducible multi-parametric estimations in the healthy human brain at 1.5T and 3T. Neuroimage. 2021;226:117573.
12. Peretti L, Donatelli G, Cencini M, et al. Generating synthetic radiological images with PySynthMRI: an open-source cross-platform tool. Tomography. 2023;9:1723–33.
13. Kurzawski JW, Cencini M, Peretti L, et al. Retrospective rigid motion correction of three-dimensional magnetic resonance fingerprinting of the human brain. Magn Reson Med. 2020;84:2606–15.
14. Donatelli G, Cecchi P, Migaleddu G, et al. Quantitative T1 mapping detects blood–brain barrier breakdown in apparently non-

enhancing multiple sclerosis lesions. Neuroimage Clin. 2023;40:103509.
15. Som PM, Lanzieri CF, Sacher M, et al. Extracranial tumor vascularity: determination by dynamic CT scanning. Part I: concepts and signature curves. Radiology. 1985;154:401–5.
16. Liebner S, Fischmann A, Rascher G, et al. Claudin-1 and claudin-5 expression and tight junction morphology are altered in blood vessels of human glioblastoma multiforme. Acta Neuropathol. 2000;100:323–31.
17. Nduom EK, Yang C, Merrill MJ, et al. Characterization of the blood-brain barrier of metastatic and primary malignant neoplasms. J Neurosurg. 2013;119:427–33.
18. Arvanitis CD, Ferraro GB, Jain RK. The blood–brain barrier and blood–tumour barrier in brain tumours and metastases. Nat Rev Cancer. 2020;20:26–41.
19. Long DM. Capillary ultrastructure and the blood-brain barrier in human malignant brain tumors. J Neurosurg. 1970;32:127–44.
20. Engelhorn T, Schwarz MA, Eyupoglu IY, et al. Dynamic contrast enhancement of experimental glioma: an intra-individual comparative study to assess the optimal time delay. Acad Radiol. 2010;17:188–193.
21. Pronin IN, McManus KA, Holodny AI, et al. Quantification of dispersion of Gd-DTPA from the initial area of enhancement into the peritumoral zone of edema in brain tumors. J Neurooncol. 2009;94:399–408.
22. Wagner S, Gufler H, Eichner G, et al. Characterisation of lesions after stereotactic radiosurgery for brain metastases: impact of delayed contrast magnetic resonance imaging. Clin Oncol (R Coll Radiol). 2017;29:143–50.
23. Ikushima I, Korogi Y, Kuratsu J, et al. Dynamic MRI of meningiomas and schwannomas: is differential diagnosis possible? Neuroradiology. 1997;39:633–38.
24. Fujii K, Fujita N, Hirabuki N, et al. Neuromas and meningiomas: evaluation of early enhancement with dynamic MR imaging. Am J Neuroradiol. 1992;13:1215–20.
25. Long DM. Vascular ultrastructure in human meningiomas and schwannomas. J Neurosurg. 1973;38:409–19.
26. Nägele T, Petersen D, Klose U, et al. The "dural tail" adjacent to meningiomas studied by dynamic contrast-enhanced MRI: a comparison with histopathology. Neuroradiology. 1994;36:303–7.
27. Hawkins CP, Munro PMG, Mackenzie F, et al. Duration and selectivity of blood-brain barrier breakdown in chronic relapsing experimental allergic encephalomyelitis studied by gadolinium-DTPA and protein markers. Brain. 1990;113:365–78.
28. Katz D, Taubenberger JK, Cannella B, et al. Correlation between magnetic resonance imaging findings and lesion development in chronic, active multiple sclerosis. Ann Neurol. 1993;34:661–69.
29. Hashemi H, Behzadi S, Ghanaati H, et al. Evaluation of plaque detection and optimum time of enhancement in acute attack multiple sclerosis after contrast injection. Acta Radiol. 2014;55:218–24.
30. Gaitán MI, Shea CD, Evangelou IE, et al. Evolution of the blood-brain barrier in newly forming multiple sclerosis lesions. Ann Neurol. 2011;70:22–29.
31. Fishman RA, Dillon WP. Dural enhancement and cerebral displacement secondary to intracranial hypotension. Neurology. 1993;43:609–609.

How to cite this article: Donatelli G, Migaleddu G, Cencini M, et al. Detection of pathological contrast enhancement with synthetic brain imaging from quantitative multiparametric MRI. J Neuroimaging. 2024;1–11.
https://doi.org/10.1111/jon.13201